HHS Public Access

Author manuscript

Proc SPIE Int Soc Opt Eng. Author manuscript; available in PMC 2020 April 27.

Published in final edited form as:

Proc SPIE Int Soc Opt Eng. 2019 February ; 10951: . doi:10.1117/12.2512996.

A deformable multimodal image registration using PET/CT and TRUS for intraoperative focal prostate brachytherapy

Sharmin Sultana, **Daniel Y. Song**, **Junghoon Lee**

Department of Radiation Oncology and Molecular Radiation Sciences, Johns Hopkins University, Baltimore, MD, USA

Abstract

In this paper, a deformable registration method is proposed that enables automatic alignment of preoperative PET/CT to intraoperative ultrasound in order to achieve PET-determined focal prostate brachytherapy. Novel PET imaging agents such as prostate specific membrane antigen (PSMA) enables highly accurate identification of intra/extra-prostatic tumors. Incorporation of PSMA PET into the standard transrectal ultrasound (TRUS)-guided prostate brachytherapy will enable focal therapy, thus minimizing radiation toxicities. Our registration method requires PET/CT and TRUS volume as well as prostate segmentations. These input volumes are first rigidly registered by maximizing spatial overlap between the segmented prostate volumes, followed by the deformable registration. To achieve anatomically accurate deformable registration, we extract anatomical landmarks from both prostate boundary and inside the gland. Landmarks are extracted along the base-apex axes using two approaches: equiangular and equidistance. Three-dimensional thin-plate spline (TPS)-based deformable registration is then performed using the extracted landmarks as control points. Finally, the PET/CT images are deformed to the TRUS space by using the computed TPS transformation. The proposed method was validated on 10 prostate cancer patient datasets in which we registered post-implant CT to end-of-implantation TRUS. We computed target registration errors (TREs) by comparing the implanted seed positions (transformed CT seeds vs. intraoperatively identified TRUS seeds). The average TREs of the proposed method are 1.98±1.22 mm (mean±standard deviation) and 1.97±1.24 mm for equiangular and equidistance landmark extraction methods, respectively, which is better than or comparable to existing state-of-the-art methods while being computationally more efficient with an average computation time less than 40 seconds.

Keywords

Deformable registration; prostate brachytherapy; PET/CT; TRUS; focal therapy

1. INTRODUCTION

Prostate cancer is the most prevalent malignancy in men and the second leading cause of cancer death in the US with approximately 164,690 new cases and 29,430 death estimated in 2018.[1] Even with current image-guidance approaches, whole prostate gland treatment is the current standard due to uncertainty and inability of defining tumor foci within the gland. However, whole-gland treatment may contribute to increased risk of toxicity. In realization of the toll on patient quality of life from current therapies, there is substantial interest

throughout the urologic oncology community in utilizing focal therapy to mitigate such toxicities.[2] The rationale for focal therapy is based upon the recognition that whole gland treatment, regardless of specific modality, is associated with unacceptable toxicity rates, while concurrently it is also realized that patient morbidity and mortality is due to the progression of major foci of high-grade disease, i.e. the index lesion.

Recent advances in multi-parametric MR imaging and more recently, PET imaging of prostate cancer have increased the potential for accurate focal therapy. Novel PET imaging agents such as PSMA have proven to be highly specific and sensitive in identification of prostate cancer, including intra/extra-prostatic tumors.[3] Most ablative treatments for prostate cancer which are considered suitable for focal therapy, including brachytherapy and cryotherapy, utilize transrectal ultrasound (TRUS) as the primary modality for image-guidance, but TRUS does not provide accurate diagnostic information regarding location of the cancer. A combination of PET with intraoperative TRUS would allow for achievement of precise focal therapy for prostate cancer. The first and key step toward successful PET-determined focal brachytherapy is the accurate registration of preoperative PET/CT and intraoperative TRUS images.

In this paper, we propose a deformable image registration algorithm for preoperative PET/CT and intraoperative TRUS image fusion. Existing multimodal image registration methods for prostate cancer mostly focus on MR-ultrasound registration for prostate biopsy. These registration algorithms can be categorized as intensity-based,[4] surface-based,[5, 6] and biomechanical model-based.[7, 8] Intensity-based methods produce inaccurate results due to poor intensity correlation between MR and TRUS images. Surface-based methods are able to accurately align the prostate boundary, but do not guarantee accurate alignment of internal structures. Biomechanical model-based approaches showed the best performance among existing methods in which deformations are constrained during the registration based on modeled and learned physical motion and tissue property. However, these approaches are computationally expensive and often require additional patient-specific training to achieve the best performance, which is cumbersome and is not suitable for intraoperative use. Similar registration approach can be used for our PET-TRUS registration in which we can use CT images taken with PET as a surrogate. However, existing algorithms need improvement in terms of registration accuracy and computational efficiency for intraoperative use.

Our PET/CT-TRUS registration algorithm uses prostate contours drawn on both CT (of PET/CT) and TRUS images similarly as the surface-based approaches. To guarantee the accurate registration inside the prostate gland, it automatically extracts landmarks from both the prostate boundary and inside the gland. A 3D thin-plate spline (TPS)-based deformable registration is then performed using the extracted landmarks. Our approach is therefore computationally fast and produce accurate registration results on both the prostate boundary and internal gland.

2. METHOD

The workflow of the proposed method is shown in Figure 1. The registration process starts with a preprocessing step followed by a rigid and finally a deformable registration. In the preprocessing step, prostate glands in both CT and TRUS images need to be contoured. PET/CT images are segmented prior to the brachytherapy procedure, and TRUS images are segmented during the planning phase of the brachytherapy procedure, i.e., routine clinical workflow. These segmentations are performed by the physician in a slice-by-slice manner. Segmented contours are smoothed by recursive Gaussian filtering to reduce stair-like effects caused by abrupt inter-slice transitions, especially in TRUS images that are typically acquired with 5 mm slice spacing.

The rigid registration is first initialized by aligning the centers of mass between the CT and TRUS prostate masks followed by rotating the CT prostate mask by an estimated TRUS probe angle to the cranial-caudal axis in the sagittal plane of the CT. This rotation adjustment is desired as the patient position between CT (supine) and TRUS (high lithotomy) are significantly different. The final rigid transformation is computed by maximizing the spatial overlap between the prostate segmentations, measured by a kappa statistics-based similarity metric.

Following the rigid registration, the deformable registration is performed which consists of two steps: 1) Automatic landmark extraction and 2) Computing the deformation using TPS.

2.1 Automatic landmark extraction

To achieve anatomically accurate registration, we extract landmarks from the prostate boundary as well as inside the gland along eight directions that are equally distributed around base-apex axis as shown in Figure 2. To determine these eight directions, we use two approaches; (1) select 8 equiangular directions around the base-apex axis and (2) select 8 points that are equally spaced along the prostate boundary from which 8 directions are determined by connecting the prostate center of mass on each slice and each selected boundary point (referred to as equidistance hereafter). For each direction, we identify a mid-gland landmark point at the half distance between the prostate center of mass and the prostate boundary point. On the prostate boundary, we add 8 additional points between the initially selected 8 points on the 8 directions to obtain similar landmark density as the mid-gland. As a result, for each 2D axial slice, a total of 25 landmark points consisting of one center of mass point, 16 prostate boundary and 8 mid-gland points are extracted.

The extracted landmarks from all slices form a 3D point cloud as shown in Figure 2. Since there are greater uncertainties in the prostate contours near the base and apex regions than the mid-gland (especially in TRUS images), we exclude the first and the last 5% of the slices along the base-apex direction. Unlike uniformly distributed landmarks or Euclidean distance-based landmarks, the extracted 3D landmark point cloud can well capture prostate shape and geometric changes in a consistent way in TRUS and CT. Intra-gland landmarks within the prostate ensure smooth transition from the prostate base-apex midline to the boundary, thus produces physically realistic registration inside the gland. The detailed steps of our landmark extraction algorithm is shown in Table 1. The registration performances of

the two landmark extraction approaches are compared, and the results are presented in the results section.

2.2 Computing the deformation using TPS

TPS is a commonly used technique to perform a smooth deformable registration based on a set of corresponding landmarks. It was originally proposed by Bookstein[9] which was a TPS interpolation between two sets of points and it was applied to 2D images. Rohr et al. then proposed an approximating TPS where an anisotropic localization error was introduced.[10], TPS and its variants have been widely used in landmark-based deformable registration.[4, 11–14]

Given a set of fixed image landmarks p_i and moving image landmarks q_i, where $i = 1, 2, \ldots, n$, n is the total number of extracted landmarks and images are of dimension d, we have to find a transformation $\mathcal{T}:\mathbb{R}^d \rightarrow \mathbb{R}^d$ between the images using two sets of landmarks p_i and q_i. The TPS-based transformation can be written as (1).

$$\mathcal{T}(x) = \sum_{V=1}^{m} a_v \phi_v(x) + \sum_{i=i}^{n} w_i U(p_i - x) \tag{1}$$

Where ϕ_V function represents the set of polynomials on, R^d, $U(r)$. is the underlying radial basis function defined as $U(r) = r^2 \log r^2$. a_V are the 12 affine coefficients of the transformation and w_i are the TPS weight coefficients which are computed solving linear system of equations.[9]

The TPS mapping between the moving and fixed landmarks can be computed by minimizing the bending energy E_{TPS} over $\mathbb{R}^3$, defined as:

$$E_{TPS} = \iiint_{R^3} \left[\left(\frac{\partial^2 \mathcal{T}}{\partial x^2}\right)^2 + \left(\frac{\partial^2 \mathcal{T}}{\partial y^2}\right)^2 + \left(\frac{\partial^2 \mathcal{T}}{\partial z^2}\right)^2 + 2\left(\frac{\partial^2 \mathcal{T}}{\partial xy}\right)^2 + 2\left(\frac{\partial^2 \mathcal{T}}{\partial yz}\right)^2 + 2\left(\frac{\partial^2 \mathcal{T}}{\partial xz}\right)^2 \right] dxdydz \tag{2}$$

Once we have computed the deformations between PET/CT and TRUS prostate masks using the sets of fixed and moving landmarks, we can apply the same deformations to the PET/CT volume to register with the TRUS volume.

3. RESULTS

We evaluated the proposed registration algorithm on 10 prostate cancer patient datasets treated by low-dose-rate (LDR) permanent brachytherapy. Each patient had intraoperative TRUS and six x-ray images acquired at the end of the seed implantation as well as a postoperative CT taken 1 day after the implantation (Day 1). From the intraoperative x-rays and TRUS images, the implanted seed locations were computed using an intraoperative registration of ultrasound and fluoroscopy (iRUF) system that our team has previously developed,[15–18] and the postoperative CT images were segmented for seed locations. Since the implanted seeds were well distributed within the prostate and their 3D coordinates were

computed in both TRUS (from intraoperative x-ray images) and CT, we used the implanted seeds as the landmarks to compute the target registration errors (TREs).

TRUS images were contoured during intraoperative treatment planning and the CT images were contoured for post-implant dosimetry. Day 1 CT was registered to the TRUS images using the proposed method. We have used a total of 250 landmarks (25 landmarks per axial slice and 10 slices across the volume). Landmarks were extracted using the equiangular and equidistance approaches as described above. Once the CT-TRUS registration was performed, the computed transformation was applied to the segmented CT seeds. TREs were then calculated by computing Euclidean distance between the transformed CT seeds and the TRUS seeds. Figure 3 shows an example registration result, and the resulting TREs of all 10 patients are reported in Table 2. The average computation time was 38 seconds on a workstation with 2.4 GHz Xeon processor with 16 GB RAM. The proposed algorithm significantly outperformed state-of-the-art methods[4, 6, 19, 20] in terms of registration error with the mean±sd (standard deviation) TREs of 1.98±1.22mm (equiangular) and 1.97±1.24mm (equidistance). We have also compared our proposed method with a distance map-based registration algorithm with B-spline regularization implemented as a module in open-source software, 3D Slicer.[21] The average TRE of this distance map-based registration for the same 10 cases was 2.68 ± 1.5 mm. The comparison result is shown in Figure 4.

4. CONCLUSIONS

This paper proposes a deformable PET/CT-TRUS registration for PET-determined focal prostate brachytherapy. PSMA PET enables identification of intra/extra prostatic tumors, thus allowing us to achieve focal therapy instead of whole-gland treatment if accurately fused with intraoperative TRUS images. The proposed registration algorithm consisting of initial rigid registration, automatic landmark extraction, and landmark-based TPS deformable registration showed accurate registration performance with computational efficiency. The proposed algorithm is simple and fully automatic except for prostate contouring. With the average registration error of less than 2 mm and average computation of 38 seconds, this method can be seamlessly incorporated into the current prostate brachytherapy procedure without adding any burden while providing critical information for focal therapy.

REFERENCES

[1]. Siegel R, Miller K, and Jemal A, [Cancer statistics, 2018 CA: a cancer. J Clin 68: 7–30], (2017).

[2]. Jain AK, and Ennis RD, “Focal therapy, differential therapy, and radiation treatment for prostate cancer,” Advances in urology, 2012, (2012).

[3]. Perera M, Papa N, Christidis D et al., “Sensitivity, specificity, and predictors of positive 68Ga–prostate-specific membrane antigen positron emission tomography in advanced prostate cancer: a systematic review and meta-analysis,” European urology, 70(6), 926–937 (2016). [PubMed: 27363387]

[4]. Mitra J, Kato Z, Martí R et al., “A spline-based non-linear diffeomorphism for multimodal prostate registration,” Medical image analysis, 16(6), 1259–1279 (2012). [PubMed: 22705289]

[5]. Yang X, Akbari H, Halig L et al., “3D non-rigid registration using surface and local salient features for transrectal ultrasound image-guided prostate biopsy.” 7964, 79642V.

[6]. Mayer A, Zholkover A, Portnoy O et al., “Deformable registration of trans-rectal ultrasound (TRUS) and magnetic resonance imaging (MRI) for focal prostate brachytherapy,” International journal of computer assisted radiology and surgery, 11(6), 1015–1023 (2016). [PubMed: 27017500]

[7]. Hu Y, Ahmed HU, Taylor Z et al., “MR to ultrasound registration for image-guided prostate interventions,” Medical image analysis,16(3), 687–703 (2012). [PubMed: 21216180]

[8]. Alterovitz R, Goldberg K, Pouliot J et al., “Registration of MR prostate images with biomechanical modeling and nonlinear parameter estimation,” Medical physics, 33(2), 446–454 (2006). [PubMed: 16532952]

[9]. Bookstein FL, “Principal warps: Thin-plate splines and the decomposition of deformations,” IEEE Transactions on pattern analysis and machine intelligence, 11(6), 567–585 (1989).

[10]. Rohr K, Stiehl HS, Sprengel R et al., “Landmark-based elastic registration using approximating thin-plate splines,” IEEE Transactions on medical imaging, 20(6), 526–534 (2001). [PubMed: 11437112]

[11]. Cool DW, Bax J, Romagnoli C et al., “Fusion of MRI to 3D TRUS for mechanically-assisted targeted prostate biopsy: system design and initial clinical experience.” 121–133.

[12]. Lu J, Srikanchana R, McClain MA et al., “Statistical volumetric model for characterization and visualization of prostate cancer.” 3976, 142–154.

[13]. Fei B, Kemper C, and Wilson DL, “A comparative study of warping and rigid body registration for the prostate and pelvic MR volumes,” Computerized Medical Imaging and Graphics, 27(4), 267–281 (2003). [PubMed: 12631511]

[14]. Xiao G, Bloch B, Chappelow J et al., “A structural-functional MRI-based disease atlas: application to computer-aided-diagnosis of prostate cancer.” 7623, 762303.

[15]. Lee J, Labat C, Jain AK et al., “REDMAPS: reduced-dimensionality matching for prostate brachytherapy seed reconstruction,” IEEE transactions on medical imaging, 30(1), 38–51 (2011). [PubMed: 20643600]

[16]. Lee J, Kuo N, Deguet A et al., “Intraoperative 3D reconstruction of prostate brachytherapy implants with automatic pose correction,” Physics in Medicine & Biology, 56(15), 5011 (2011). [PubMed: 21772077]

[17]. Kuo N, Dehghan E, Deguet A et al., “An image-guidance system for dynamic dose calculation in prostate brachytherapy using ultrasound and fluoroscopy,” Medical physics, 41(9), (2014).

[18]. Dehghan E, Lee J, Fallavollita P et al., “Ultrasound–fluoroscopy registration for prostate brachytherapy dosimetry,” Medical image analysis, 16(7), 1347–1358 (2012). [PubMed: 22784870]

[19]. Hu Y, Gibson E, Ahmed HU et al., “Population-based prediction of subject-specific prostate deformation for MR-to-ultrasound image registration,” Medical image analysis, 26(1), 332–344 (2015). [PubMed: 26606458]

[20]. Fedorov A, Khallaghi S, Sánchez CA et al., “Open-source image registration for MRI–TRUS fusion-guided prostate interventions,” International journal of computer assisted radiology and surgery, 10(6), 925–934 (2015). [PubMed: 25847666]

[21]. Fedorov A, Beichel R, Kalpathy-Cramer J et al., “3D Slicer as an image computing platform for the Quantitative Imaging Network,” Magnetic resonance imaging, 30(9), 1323–1341 (2012). [PubMed: 22770690]

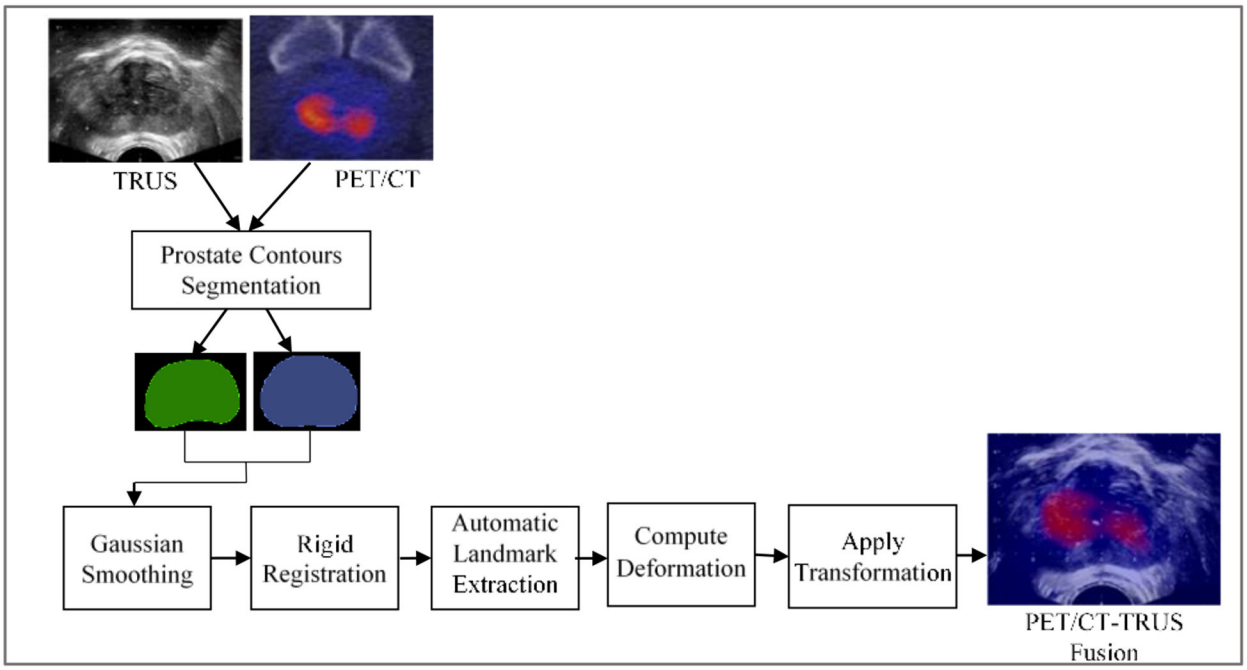

Figure 1.
PET/CT-TRUS registration workflow.

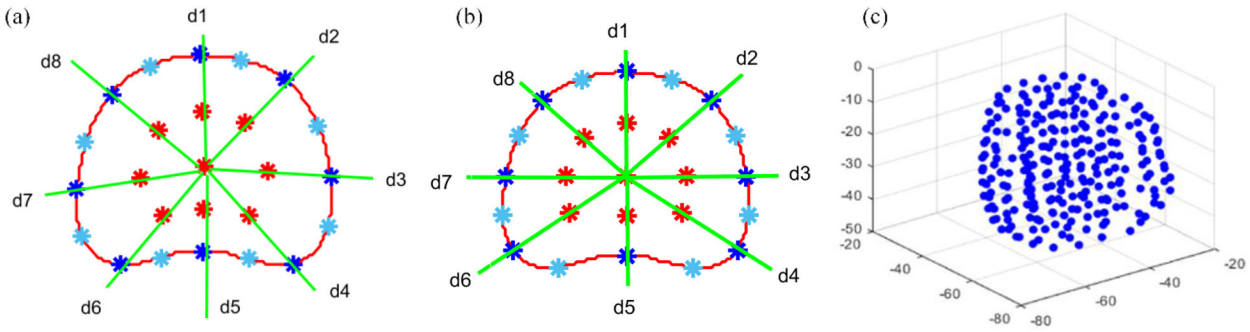

Figure 2.

Landmark extraction. An example axial slice with extracted landmarks based on (a) equidistance and (b) equiangular approaches. In each axial slice, one center of mass point, 8 mid-gland (red) and 8 prostate boundary (blue) points, and 8 additional points on the prostate boundary (light blue) are extracted. (c) Extracted 3D landmarks.

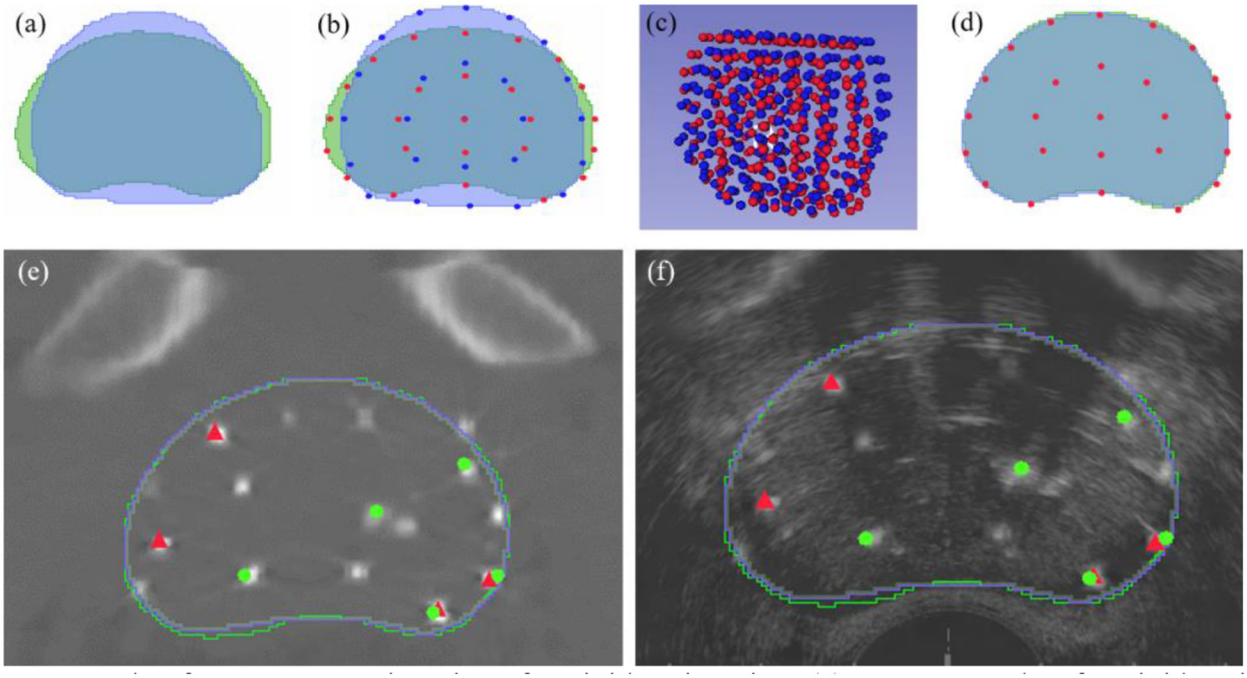

Figure 3.

An example of CT-TRUS registration after rigid registration. (a) Prostate masks after rigid registration. Green: TRUS prostate mask. Blue: CT prostate mask. (b) Extracted landmarks. Red: TRUS landmarks. Blue: CT landmarks. (c) 3D landmarks. (d) Registered CT and TRUS masks overlapping area is shown as teal color and all landmarks are matched (shown as red). (e) TRUS seeds (red triangle) and registered CT seeds (green dots) are superimposed on a registered CT image and (f) TRUS image. The matching of CT and TRUS seeds with the bright white dots indicate that the CT and TRUS volumes are well registered.

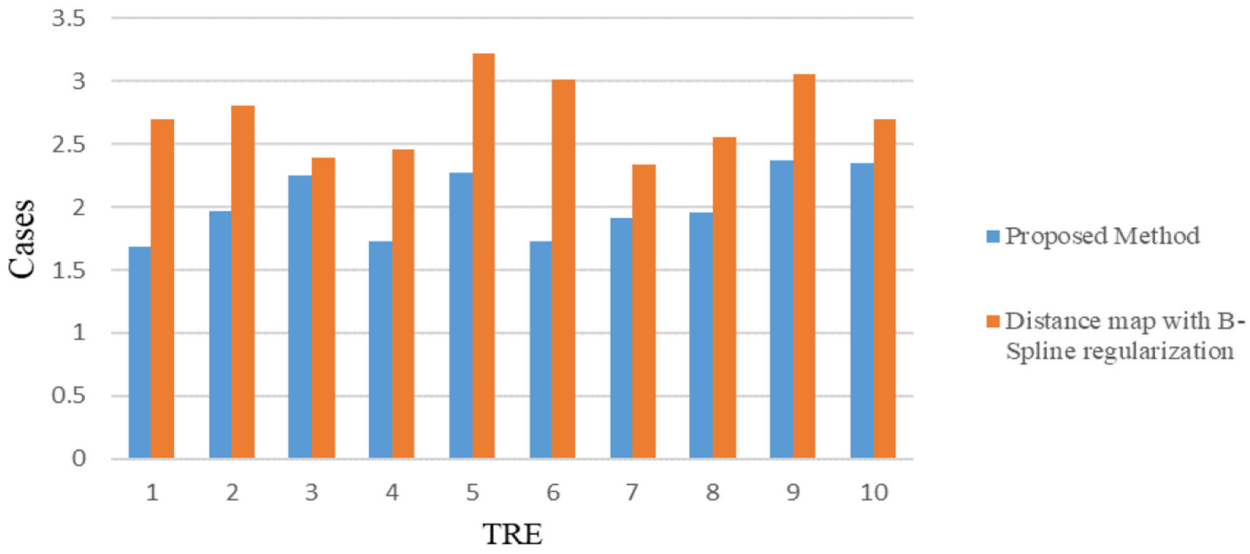

Figure 4.
Registration performance comparison between the proposed method and a distance-map-based registration technique

Table 1.

Landmark Extraction Algorithm

For slice 1 to N

1 Compute the prostate center of mass, C_i.

2 Find 8 radial lines, starting from center towards the boundary.

3 For each radial line,

a. Find the intersection point between the radial line and the boundary (boundary landmarks BW_i).

b. Find the mid-point between C_i and BW_i (intra-gland landmarks).

c. Find 8 mid-points between adjacent BW_i's (additional boundary landmarks).

Table 2

TREs of CT-TRUS registration for 10 cases.

Case	Number of Seeds	Equiangular landmarks TRE (mm) mean±sd (max)	Equidistance landmarks TRE (mm) mean±sd (max)
1	101	1.50±1.02 (4.74)	1.55±1.25 (6.61)
2	66	2.00±1.00 (4.25)	2.20±1.18 (4.52)
3	78	2.33±1.56 (6.41)	2.30±1.30 (7.35)
4	78	1.62±0.85 (5.86)	1.64±0.95 (6.44)
5	76	2.30±1.16 (7.26)	2.34±1.20 (5.71)
6	104	1.80±1.22 (5.83)	1.82±1.25 (6.81)
7	78	2.17±1.94 (7.60)	2.12±1.95 (7.20)
8	61	2.44±1.42 (6.53)	2.30±1.40 (6.30)
9	103	1.74±0.99 (5.73)	1.75±0.95 (5.80)
10	97	1.91±1.05 (4.83)	1.70±0.98 (4.20)
Average	84	1.98±1.22 (7.60)	1.97±1.24 (7.35)